Statics and dynamics of an interface in a temperature gradient

D. Boyanovsky,[1] David Jasnow,[1] J. Llambías,[1] and F. Takakura[1,2]
[1] *Department of Physics and Astronomy, University of Pittsburgh, Pittsburgh, Pennsylvania 15260*
[2] *Universidade Federal de Juiz de Fora, Instituto de Ciencias Exatas, Departamento de Fisica, Juiz de Fora, Minas Gerais, Brazil*
(Received 22 November 1994)

Here we are primarily concerned with the effect of a (normally oriented) temperature gradient on an equilibrium interface separating coexisting phases in a symmetric binary system below its critical temperature. In such a system, the temperature couples "weakly" to the order parameter and does not favor either of the potentially coexisting bulk phases. Nonetheless, for a large system, there can be a dramatic effect and a failure of a linear response owing to the breaking of translational invariance by the spatially varying temperature. Two types of boundary conditions on the order parameter, natural and "topological," are used. The structure of the effective free energy, nonconserved dynamics, and the Langevin equation for the collective coordinate specifying the interface position are analyzed.

PACS number(s): 05.70.−a, 64.90.+b, 68.10.−m

I. INTRODUCTION

Thermocapillarity effects, in which the interfacial properties of two phase systems provide the dominant driving forces and control flows and motion, are of interest in a variety of areas [1]. These include two-phase flows, droplet migration, and a variety of other phenomena in a microgravity environment (see, e.g., Ref. [2]), and, for example, convection in which the Marangoni effect plays a determining role (see, e.g., Ref. [3] and references cited therein). To gain a deeper understanding of these and other phenomena, it is of interest to consider the effect of a temperature gradient on a two-phase interface within a coarse-grained description.

In this paper we study static and dynamic aspects of the response of the interface separating two coexisting phases in a symmetric binary system below its critical temperature to an imposed temperature gradient. In such a model the spatially varying temperature couples "weakly" to the order parameter and, in any region, does not favor one or the other of the potentially coexisting phases. Nonetheless, the effect of the perturbation can be strong because of the breaking of translational invariance. In the dynamics considerations, we restrict ourselves here to the case of a nonconserved order parameter.

While the model we will consider is just a first step in dealing with the fluid systems mentioned above, this work does have potential relevance to the understanding of transport phenomena mediated by solitons in systems with nonuniform temperature. The reason for this is that, as we will see below, a temperature gradient drives the interface out of equilibrium thus modifying the dynamics of the soliton. Hence this mechanism may have implications in charge transport, and our analysis may be of interest in charge-density wave systems [4] and quasi-one-dimensional organic polymers [5] and other mesoscopic condensed matter systems in which solitons play an important role [6]. In particular, our analysis applies directly to a coarse-grained description of charge density wave excitations in quasi-one-dimensional chains [7].

To deal properly with fluid phenomena, for example the migration of a droplet of one phase in the background of its coexisting partner, the dynamics treated here must be generalized to include order parameter conservation as well as flow. This is beyond the present scope. Solidification phenomena, on the other hand, require a different coupling of the temperature variable to the order parameter than will be considered here.

We approach the question of the effect of nonuniform temperature from both analytic and numerical directions. The analysis presented here essentially addresses the nature of the free energy of a two-phase interface (or kink) in a temperature gradient. Accordingly, the dynamics addressed here are restricted to a nonconserved order parameter.

We find interesting features in the behavior. In particular, a temperature gradient couples to the the so-called "translation" mode of the interface which is then only weakly clamped by the finite size of the system. We find that a perturbative analysis has a vanishing domain of applicability in a large system, i.e., linear response fails. The structure of the effective free energy as a function of the collective coordinate describing the interface position is sensitive to the boundary conditions, but kinks not too near the boundaries are seen to move with constant velocity linear in the gradient. Kink solutions in the simplest situations are commonly represented as solutions of mechanical equations describing a ball rolling down a hill. In the presence of a temperature gradient, we show that a mechanical analog still holds, but now the ball rolls with friction.

The remainder of this paper is organized as follows. In Sec. II the statics of a nonconserved order parameter in a temperature gradient are considered, while in Sec. III effective Langevin dynamics for the collective coordinate describing the interface position are derived. A

comparison with a full numerical analysis using relaxational (model A in the lexicon of Ref. [8]) dynamics is included. Section IV is reserved for concluding remarks.

II. STATICS

We consider a coarse-grained description of system allowing a transition from a single phase to a state of two-phase coexistence with a scalar order parameter, ϕ. The temperature is allowed to vary slowly along one particular direction (chosen to be x) inside the sample, which is confined in a box $0 \leq x \leq L$. We consider configurations translationally invariant in directions perpendicular to the gradient. For a configuration $\phi(x)$ the free energy per unit "area" is taken to be

$$F = \int_0^L dx \left[\frac{1}{2} \left(\frac{\partial \phi(x)}{\partial x} \right)^2 - \frac{1}{2} r^2(x) \phi^2(x) + \frac{\lambda}{4} \phi^4(x) \right] . \tag{2.1}$$

In such a model the function $r^2(x)$ can be taken to specify the local temperature difference from a reference (critical) temperature. We take the temperature to be slowly varying and parametrize

$$r(x) = r_0 \left(1 + \frac{\Delta r}{r_0 L} x \right) . \tag{2.2}$$

This parametrization will prove to be convenient for the analysis to follow. Furthermore, for $\Delta r / r_0 \ll 1$, which will be the case of interest, the temperature varies almost linearly with distance, with $x = 0$ being the hotter and $x = L$ the colder ends of the sample. While our explicit calculations and simulations are for the specific model described above, general features of the results are not expected to depend on the details of the free-energy functional. Note that $r(x) > 0$ throughout the sample, keeping the system below critical everywhere, and that for the particular coupling in Eq. (2.1) neither of the two potentially coexisting phases is locally favored. The coupling of the temperature to the order parameter is appropriate to phase separation and does not describe solidification.

Equilibrium configurations are extrema of the free energy functional (2.1), which leads to the search for solutions to the following nonlinear differential equation:

$$-\frac{\partial^2 \phi(x)}{\partial x^2} - r^2(x) \phi(x) + \lambda \phi^3(x) = 0 . \tag{2.3}$$

Notice that with the particular choice (2.2), $\phi(x) = \pm r(x)/\sqrt{\lambda}$ is an exact solution of (2.3) corresponding to a particular local equilibrium configuration. It proves convenient to remove the local equilibrium variation and to introduce a nonlinear change of variables

$$\phi(x) = \frac{r(x)}{\sqrt{\lambda}} \eta(z(x)) \tag{2.4}$$

and the dimensionless parameter

$$h = \frac{\Delta r}{L r_0^2} \tag{2.5}$$

with $h \ll 1$. (Variable changes of this type are frequently used within the context of nonlinear differential equations and discussed in Ref. [9].) This parameter measures the strength of the temperature gradient. The dependence of $z(x)$ is determined by requiring that the coefficient of the $d^2\eta/dz^2$ in the resulting differential equation for $\eta(z)$ be unity. This requirement yields the simple relation

$$\frac{dz(x)}{dx} = r(x). \tag{2.6}$$

We furthermore impose the boundary condition $z(0) = 0$ thus obtaining the new dimensionless variable

$$z(x) = r_0 x + \frac{h}{2} (r_0 x)^2 \tag{2.7}$$

measuring the "distance" from the hot wall. With the assumption that $\Delta r / r_0 \ll 1$ and hence $h, hLr_0 \ll 1$, the differential equation for $\eta(z)$ in terms of the new dimensionless variable z becomes

$$\ddot{\eta} + 3h\dot{\eta} + \eta - \eta^3 = 0 \tag{2.8}$$

where dots stand for derivatives with respect to z. For $h = 0$ there are well known "kink" solutions to this equation (see e.g., Ref. [10]).

The advantage of parametrizing $r(x)$ as in (2.2) and of the change of variables (2.4) becomes clear. Whereas in the original differential equation (2.3) the x dependence of $r(x)$ broke explicit translational invariance, the differential equation for $\eta(z)$ is *manifestly* translational invariant in the variable z. Furthermore, Eq. (2.8) provides a very appealing physical interpretation: $\eta(z)$ describes the position of a particle moving at "time" z in a potential

$$V(\eta) = \frac{1}{2}\eta^2 - \frac{1}{4}\eta^4 \tag{2.9}$$

damped by velocity-dependent friction proportional to h. The present work involves analysis of Eq. (2.8).

Before searching for solutions to the differential equation, we must specify boundary conditions. Since we are interested in the behavior of interfaces, relevant boundary conditions are those compatible with solutions that have one node (the position of the interface). We will focus on two sets of boundary conditions. The first, type I, corresponds to natural boundary conditions:

$$\text{type I:} \quad \left. \frac{d\phi(x)}{dx} \right|_{x=0} = 0 \ ; \ \left. \frac{d\phi(x)}{dx} \right|_{x=L} = 0. \tag{2.10}$$

The corresponding conditions on $\eta(z)$ at $z = 0$ and $z = l \equiv z(x = L)$ are $\dot{\eta}(z = 0, l) = -h\eta(z = 0, l)$. Note we always will consider $hLr_0 << 1$.

In the boundary conditions of type II, the order parameter is fixed at the "local equilibrium" values, namely,

$$\text{type II:} \quad \phi(0) = \mp \frac{r(0)}{\sqrt{\lambda}} \ ; \ \phi(L) = \pm \frac{r(L)}{\sqrt{\lambda}} \tag{2.11}$$

corresponding to $\eta(0) = \mp 1$; $\eta(l) = \pm 1$.

A. Boundary conditions I

1. *Perturbative solutions*

For these boundary conditions there is surely a solution in which the order parameter remains in one phase, with the $|\eta| \simeq 1$. We refer to this as the local equilibrium solution, which will be a global minimum of the free energy functional. For small h a perturbative solution is easily found with $\eta(z) = -1 + \delta(z)$ and $\delta(z) = e^{-\frac{3}{2}hz}[A\cosh(Wz) + B\sinh(Wz)]$, with A, B chosen to satisfy the boundary conditions and $W = \sqrt{2 + \frac{9}{4}h^2}$.

Having established the configuration with the lowest free energy for the case of boundary conditions (I), we now concentrate on finding a solution with an interface. This solution must necessarily have one node, and for very small h we expect that its behavior away from the node will have $|\eta| \simeq 1$.

For $h = 0$, the solution $\eta_0(z)$ may be found by quadratures in terms of the elliptic sine function [11,12]. Since the problem of an interface or "kink" in a finite system is not standard, we present some useful properties of the solution to the unperturbed problem in Appendix B. These properties are important in obtaining a perturbative solution in the presence of the temperature gradient. For $h \neq 0$ there are no exact solutions to the differential equation, which in its original form (2.3) may be recognized (for $h \ll 1$) as a Painlevé transcendental without an exact solution [9]. Although this is a formal property, one of its main consequences is that the solution is nonsingular in a finite interval [9] (the only possible singularities are at infinity), and this suggests that a perturbative approach may be feasible, namely, letting

$$\eta(z) = \eta_0(z) + h\eta_1(z) + \cdots . \tag{2.12}$$

This expansion will allow us to study the linear response of the interface profile to the temperature gradient.

We now need to find the first order correction η_1. This function obeys the linearized equation

$$\ddot{\eta}_1 + \eta_1 - 3\eta_0^2\eta_1 = -3\dot{\eta}_0 . \tag{2.13}$$

This shows that the temperature gradient couples to the "translation mode" of the system, $\delta_1 \equiv \dot{\eta}_0$, which satisfies the homogeneous equation in Eq. (2.13). The existence of this mode yielding zero eigenvalue for the fluctuation operator ($\mathcal{L} = d^2/dz^2 + 1 - 3\eta_0^2$) is a direct result of translational invariance (see, e.g., Ref. [13]). This can be seen as follows: in the absence of the temperature gradient, the free energy functional is translationally invariant (in the infinite volume limit). A displacement of the position of the interface $\eta(z) \to \eta(z+a) \approx \eta(z) + a d\eta/dz$ (with a a constant) does not cost free energy. Thus $d\eta(z)/dz$ is an eigenvector of the small fluctuation operator $\mathcal{L}$ with zero eigenvalue [10]. Were it not for the fact that the domain is finite, such a perturbative analysis could not be carried out. In the present case a solution can be constructed using elementary methods. A particular solution of Eq. (2.13) is obtained in a standard manner from the two linearly independent solutions of the homogeneous equation. As mentioned above, translational invariance guarantees that δ_1 is a solution of the homogeneous equation. From this solution we can construct another linearly independent solution of the homogeneous equation, δ_2, with unit Wronskian. From these two solutions the particular solution can be obtained; however, this solution will not obey the proper boundary conditions. The solution that we seek is found by adding a solution of the homogeneous equation to the particular solution fixing the coefficients to enforce the boundary conditions. The steps leading to the final form of the solution that obeys the proper boundary conditions are included in Appendix A. As one might expect, near $Z = z - l/2 \simeq 0$ the solution is of the form

$$\eta(Z) = \eta_0(Z) + h\alpha_1 \frac{d\eta_0(Z)}{dZ} + \cdots \approx \eta_0(Z + h\alpha_1) + \cdots , \tag{2.14}$$

where the constant α_1 (see Appendix A) is determined by the boundary conditions, and the terms indicated by dots vanish at $Z = 0$. Clearly the position of the interface has been shifted to $Z = -h\alpha_1$ [i.e., $z = (l/2) - h\alpha_1$]; it remains to calculate α_1. A perturbative analysis will be possible as long as $h\alpha_1$ is sufficiently small.

The explicit evaluation of η_1 is, in general, complicated by the unwieldy elliptic functions and elliptic integrals. However, it is simplified in the physically relevant large volume limit. Some background is provided in Appendix B. Since we want only one node of the order parameter profile, this requires that the half-period of the elliptic function that corresponds to the unperturbed solution (B1) becomes very large in the large volume limit. After some tedious but straightforward algebra we find that

$$\alpha_1 \approx -\frac{\sqrt{2}}{64} e^{\sqrt{2}l}. \tag{2.15}$$

This is one of the main results of this paper. Before proceeding it is useful to consider the perturbative correction in the case of small amplitudes. That is, one may linearize Eq. (2.8) near $\eta \approx 0$, discarding the cubic term. Although in this approximation the differential equation describes an (underdamped) harmonic oscillator, the linear response field $\eta_1(Z)$ can be compared to the exact solution. Requiring that there be only one node in the interval requires that $l = \pi$ [the asymptotic limit of the elliptic integral $K(m)$; see Appendix B]. The first order correction η_1 agrees with the first order term (in h) in the expansion of the exact solution with boundary conditions of type I. The amplitude of the perturbation is of order hl, and the perturbative analysis is reliable whenever $hl \ll 1$, corresponding physically to the gradient being small on the scale of the correlation length. Ultimately secular terms destroy the approximation as hl becomes too large. The situation is much worse in the nonlinear case to which we now return.

The result contained in Eq. (2.15) is important: the coefficient that determines the translation of the interface becomes exponentially large in the large volume limit, signaling the breakdown of perturbation theory and lin-

ear response analysis. The relevant combination can be seen from Eq. (2.14) to be $h\alpha_1$. Furthermore, the sign of the coefficient shows that the interface is shifted dramatically toward the colder end. This suggests that the extremum found does not correspond to a local minimum of the free energy functional. However, the result is physically reasonable. The temperature gradient breaks translational invariance; this is the reason that it couples to the "zero mode," i.e., the direction in function space associated with translational displacement. In the very large volume limit the translation mode is only weakly clamped by the boundaries, therefore its coupling to the temperature gradient results in a large shift of the interface under the perturbation.

2. *Numerical results*

Since exact analytical solutions are not generally available and perturbation theory leads to an exponentially divergent linear response to the temperature gradient, we obtained numerically the profiles for the order parameter using a shooting method to solve the differential equation with type I (natural) boundary conditions given in Eq. (2.10).

Figure 1 shows the $\eta(z)$ vs z for $h = 10^{-3}$ for a system of size $l \approx 40$. We clearly see that the perturbed interface is established near the cold end of the sample, forming a boundary layer of about two correlation lengths. (In dimensionless units, the correlation length is $\xi \approx \sqrt{2}$.) From the numerical standpoint and the interpretation of $\eta(z)$ as the trajectory of a particle rolling down the potential (2.9) under constant friction $h \ll 1$, the reason that the extremum configuration has an interface close to the cold end in the large volume limit $l \gg \xi$ is clear.

The initial condition for "shooting," that is, the value

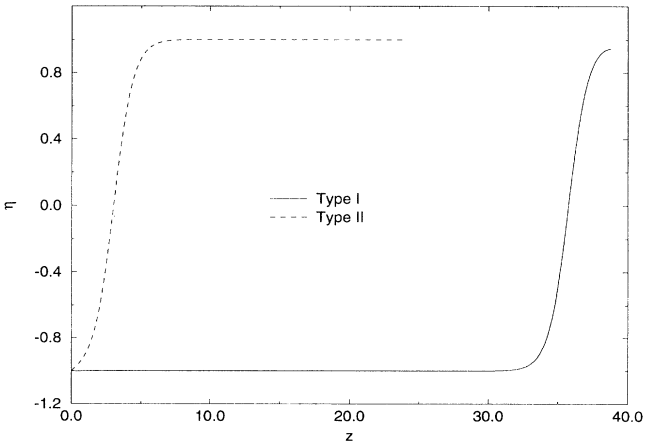

FIG. 1. Solid line: $\eta(z)$ vs z; $h = 10^{-3}$; $l \approx 40$ with boundary conditions (I), showing the extremum solution with the interface near the cold boundary. Dashed line: $\eta(z)$ vs z; $h = 10^{-3}$; $l \approx 25$ with boundary conditions (II), showing the extremum (global equilibrium) solution with the interface near the hot boundary.

of $\eta(0)$ for the boundary condition $\dot{\eta}(z)|_{z=0} = -h\eta(0)$, must be such that $\eta(0) < -1$; $\dot{\eta}(0) > 0$. In this manner, the particle first has to climb up the potential hill to $\eta = -1$ and reach that point with an extremely small velocity, remaining for a long time around that point and slowly falling down on the other side of the potential maximum. It then increases its velocity, passes through $\eta = 0$, and climbs up the potential hill toward $\eta = +1$. Because of friction, the velocity reaches zero before reaching the top, and the particle turns back; the integration stops when the boundary condition is obeyed again, now with negative velocity. On the other hand, if the integration were begun with $\eta(0) > -1$, for a large volume there would only be solutions with many nodes corresponding to a higher free energy. A solution with only one node and $\eta(0) > -1$ will only appear for small volumes, compatible with the solution found in the linearized region near $\eta \approx 0$.

Thus in the large volume limit, the particle must begin with $\eta(0) < -1$ (the "antikink" solution will begin with $\eta(0) > 1$) with a small upward velocity given by the boundary condition and will remain near the local equilibrium region $\eta \approx -1$ for most of the time, making a rather quick transition near the cold end $z \approx l$. However unlike in the topological "kink" case, the solution with one interface is in the same sector in functional space as the local equilibrium solution in that it has the same boundary conditions (of type I). But clearly the local equilibrium solution corresponds to the lowest free energy among the functions with such boundary conditions. The solutions to the differential equations (2.3) and (2.8) are indeed extrema of the free energy functional; the solution with one interface cannot be a local maximum because adding "wiggles" in the configuration will increase the free energy via the derivative terms.

If the configuration were a *local* minimum with a free energy higher than the local equilibrium solution, then there must be a local maximum that separates the two solutions. However, there is no evidence of another solution with the same boundary conditions. This reasoning leads us to conjecture that the solution with the interface is most likely a saddle point of the free energy functional. To prove this conjecture, we would have to study the spectrum of fluctuations around this solution with an interface and identify a particular direction in function space for which an eigenvalue is negative. In the present case this is an extremely difficult problem complicated by the boundary conditions on the solution.

In the case of zero temperature gradient and in the large volume limit, because of translational invariance, a shift of the interface costs negligible free energy (when the interface is far from the boundaries). With the temperature gradient, translational invariance is broken and there is a profile which extremizes the free energy. Thus our strategy is to propose a good trial "kinklike" function parametrized by the position of the interface z_c and to compute the free energy as a function of this parameter. This is equivalent to treating the position of the interface as a "collective coordinate," which is appropriate in the case of kinks and identifies the coordinate, z_c, as the translational degree of freedom [13–15].

We have found for a wide range of parameters h and l that the numerical solution to the differential equation (2.8) is very well described by the interpolating function

$$\eta(z,z_c) \approx \left(1+\frac{h}{\sqrt{2}}\right)\tanh\left[\frac{z-z_c}{\sqrt{2}}\right]. \tag{2.16}$$

Here z_c determines the position of the interface. The accuracy of this fitting function is better than 1% in most of the volume, with slightly larger departures of about $2-3\,\%$ near the boundaries of the sample, but extremely accurate near the interface. In terms of $\eta(z;z_c)$ and the variable z, the free energy as a function of z_c is given by [up to linear order in h consistently with our expansion of the differential equation (2.8)]

$$F[z_c] \approx \left(\frac{r_0^3}{\lambda}\right)\int_0^l dz(1+3hz)\left\{\frac{1}{2}\left(\frac{d\eta(z;z_c)}{dz}\right)^2 -\frac{1}{2}\eta^2(z;z_c)+\frac{1}{4}\eta^4(z;z_c)\right\} +\frac{h}{2}\left[\eta^2(l;z_c)-\eta^2(0;z_c)\right]. \tag{2.17}$$

It is clear from this expression that in terms of the field η and the variable z, the breakdown of translational invariance is in the metric (and for large enough system, weakly from the boundaries).

Figure 2 shows $F[z_c]$ vs z_c for $h = 10^{-3}$, $l \approx 40$ obtained by using (2.16); these values of the parameters are the same as those for Fig. 1 (type I boundary conditions). We see that $F[z_c]$ has a *maximum* at $z_c = z_{\max} \approx 36$ whereas the "shooting" numerical integration gives the value of the position of the interface (i.e., the node, $\eta = 0$) at $z_c = 35.8$, giving confidence that the full numerical approach yields a solution corresponding to this maximum. Except within a few correlation lengths of the boundaries, we find that $F[z_c]$ varies approximately linearly with the interface position z_c with a slope

$$\frac{dF[z_c]}{dz_c} = \left(\frac{r_0^3}{\lambda}\right)2\sqrt{2}h + O(h^2) + \cdots = 3h\sigma_0 + O(h^2) + \cdots, \tag{2.18}$$

where $\sigma_0 = r_0^3 2\sqrt{2}/3\lambda$ is recognized as the interfacial free energy (surface tension) for an interface when $h = 0$. We will compare this to our dynamical simulations described below.

These and other numerical consistency checks between the trial function approach and the full nonlinear solution lead us to conclude that the configuration that extremizes the free energy with one interface (node) corresponds to a *maximum* in the functional direction corresponding to translations, and is thus interpreted as a saddle point configuration. This saddle already exists for the unperturbed case ($h = 0$) under the boundary conditions of type I, and the situation for small h represents a smooth deformation.

If this interpretation is correct, there emerges the question as to the identification of the thermodynamically different states separated by this saddle. These states should be global minima of the free energy functional, because if one were a global and the other a local minimum, there should then be additional solutions of the differential equation with different free energies. However, as mentioned above, we find only two: the local equilibrium solutions (near $\eta = \pm 1$) and the interface solution. Thus our conclusion is that the saddle point separates the thermodynamically different states corresponding to the (nodeless) local equilibrium solutions near $\eta = \pm 1$, which are degenerate. This interpretation will be strengthened by the study of the dynamics in the next section.

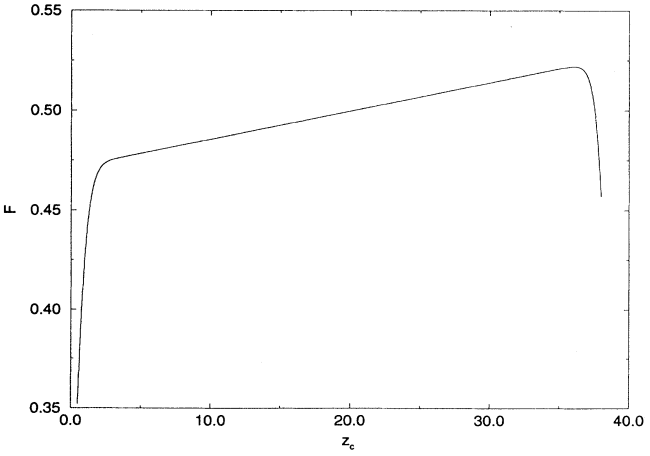

FIG. 2. $F[z_c]$ vs z_c for $h = 10^{-3}$; $l \approx 40$ with the parametrization (2.16).

B. Boundary conditions of type II

1. *Perturbative analysis*

These are "topological" boundary conditions that force the order parameter to have at least one node, and clearly there is no equivalent of the local equilibrium configuration (in which the order parameter maintains the same sign) that is available with boundary conditions I. Hence we expect that the single-node solution of the differential equation (2.8) with boundary conditions of type II is thus an absolute minimum of the free energy in the space of functions with these boundary conditions. Before analyzing the solution numerically, it proves illuminating to study the linear response as in the previous case. For sufficiently large volumes an excellent approximation to the unperturbed solution ($h = 0$) is $\eta_0(Z) = \tanh[Z/\sqrt{2}]$. With this unperturbed solution we can explicitly construct the functions $\delta_1(Z)$; $\delta_2(Z)$ and the response field η_1 satisfying $\eta_1(-l/2) = \eta_1(l/2) = 0$ (see Appendix A). Again because the boundary conditions are symmetric, the coefficient α_2 vanishes, and we find (for $l \gg 1$)

$$\alpha_1 \approx \frac{e^{\sqrt{2}l}}{16}. \tag{2.19}$$

Perturbation theory has a vanishing domain, but an important feature is that, in contrast with the previous case, now α_1 is *positive*. This means that in this case the perturbed interface lies closer to the hot end of the sample.

2. Numerical results

We have used the same numerical scheme to solve the full nonlinear differential equation (2.8), now beginning with $\eta(0) = -1$ and "shooting" with an initial derivative such that $\eta(l) = 1$. Figure 1 also shows the profile for $h = 10^{-3}$; $l = 25$ (type II boundary conditions).

The profile is again easily understood in terms of the particle rolling down the potential hill in the presence of friction: the particle has to begin from $\eta(0) = -1$ but with a fairly large derivative because of the friction term. If the initial velocity is small, then the particle does not make it up the hill to reach $\eta = 1$. Thus the initial velocity is fairly large and the particle moves very rapidly initially taking a short time to reach $\eta = 0$; hence the interface is very close to $z = 0$, the hot end. Eventually the particle climbs up the potential hill, being slowed down not only by the potential but also by the friction.

One knows that, because of the coupling to the translation mode, the linear response must necessarily diverge in the infinite volume limit. Here, for a large but finite system, the position of the perturbed interface is very close (about two to three correlation lengths) to the hot end, far from the unperturbed value at the middle of the system. The sign of the translation is correctly predicted by the linear response calculation as is the case for boundary conditions of type I. However, unlike the case of type I boundary conditions, this solution, as discussed above, corresponds to the lowest free energy compatible with the odd boundary conditions of type II.

III. DYNAMICS

A. Langevin equation for the collective coordinate

Below we will present the results of simulations of relaxational dynamics for the motion of a two phase interface in a temperature gradient. Before doing so, we derive from the trial function (2.16) the velocity of the interface.

Relaxational dynamics for this nonconserved order parameter are specified by assuming a Langevin equation description

$$\frac{\partial\phi(x,\tau)}{\partial\tau} = -\frac{\delta F}{\delta\phi}. \tag{3.1}$$

For our present purposes we neglect a noise term and absorb the characteristic relaxation rate into the dimensionless time, τ. Assuming that there is a very small distortion of the profile as a function of time, that is, that the time evolution corresponds to translations of the interface, we propose the parametrization

$$\phi(x,\tau) = \frac{r(z)}{\sqrt{\lambda}}\eta(z - z_c(\tau)) \ . \tag{3.2}$$

This parametrization leads at once to an equation for the "collective coordinate" $z_c(\tau)$. For $\xi \ll z_c \ll l$ and $h \ll 1$ and using the trial function (2.16) we find

$$\frac{dz_c}{d\tau} = -3r_0^2 h + O(h^2) + \cdots \ . \tag{3.3}$$

The interface is predicted to move with constant speed proportional to the gradient; in the language of solitons the coefficient would be identified as the kink (linear) mobility. Details are compared directly with the results of simulations below.

B. Numerical simulation

We follow the time evolution of the system using the Langevin dynamics, (3.1). These dynamics drive the system to a free energy minimum. Rescaling $\phi = \phi_0\phi'$, $x = x_0x'$, and $\tau = \tau_0 t$, one can choose the constants ϕ_0, x_0, τ_0 to reduce the dynamical equation to

$$\frac{\partial\phi(x,t)}{\partial t} = \frac{\partial^2\phi(x,t)}{\partial x^2} + (1+hx)^2\phi(x,t) - \phi^3(x,t), \tag{3.4}$$

where we use the same symbols for the rescaled variables for simplicity. The only parameter remaining is h, which corresponds, as above, to a temperature gradient, such that temperature decreases with increasing x if h is positive.

Equation (3.4) was numerically integrated using a simple Euler discretization on a one-dimensional lattice of 100 nodes with mesh size $\Delta x = 0.1$ and time step $\Delta t = 0.001$. We considered separately the two types of boundary conditions discussed above. In type I, the order parameter ϕ was required to have zero gradient at the boundaries by imposing reflecting boundary conditions. In the second case (type II), the value of the order parameter was fixed at the boundaries, with values corresponding to a different phase at each end of the sample. The value chosen was the equilibrium order parameter for an isothermal system at the temperature corresponding to that point. (This corresponds to $\eta = \pm 1$ in the earlier parametrization.) The initial conditions used were of the form

$$\phi(x,0) = (1+hx)\tanh\left[\frac{x-x_0}{\sqrt{2}}\right], \tag{3.5}$$

where x_0 is the initial position of the kink. This function is very close to the actual values that the order parameter takes once it enters the dynamic regime, as long as x_0 is not too close to the boundaries.

For the open boundary case (type I), it was observed that the evolution of the system consists of the kink being displaced until it disappears at one of the boundaries.

The final state is then always a single phase in the whole system, and at that point there is no further change in the order parameter. This type of solution has been referred to above as the "local equilibrium" configuration. This is expected, since the one-phase configuration constitutes the global minimum of the free energy, and it can be reached with the imposed boundary conditions.

For most initial positions the kink moves towards the higher temperature side. This is to be expected since near the high temperature side the correlation length is larger and the equilibrium order parameter gap is smaller. These effects decrease the interfacial free energy so that the kink can evolve to a lower free energy state by moving toward the hot end. However, it is interesting that if the initial kink position is close enough to the cold boundary, the kink disappears at that end. Figures 3(a) and 3(b) show the evolution of the kink when it is started from two different positions; in all cases the kink disappears at the boundary. This can be understood by looking at the free energy of the system as a function of the kink position $x_0(t)$, defined as the point where the order parameter vanishes. The free energy has a maximum at some value of x_0 close to the cold end. The larger the temperature gradient h, the closer this maximum is to the cold end. Figure 4 shows this free energy as a function of the kink position. It was calculated from Eq. (2.1) applied to the the order parameter configuration as the kink evolves. For a given initial condition, we can obtain only a portion of the graph as the interface evolves toward one side. However, for different initial conditions, the calculated free energy always falls on the same curve, as expected.

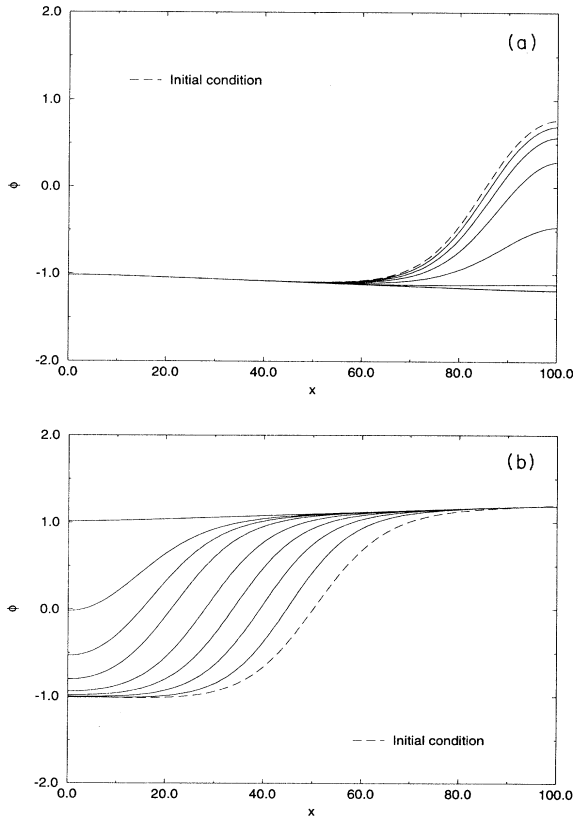

FIG. 3. (a) Evolution of structure with initial interface near the cold boundary showing the disappearance of the interface there. (b) Dynamical evolution of an interfacial structure showing the disappearance of the interface at the hot boundary. The value $h = 0.002$ was used in these figures.

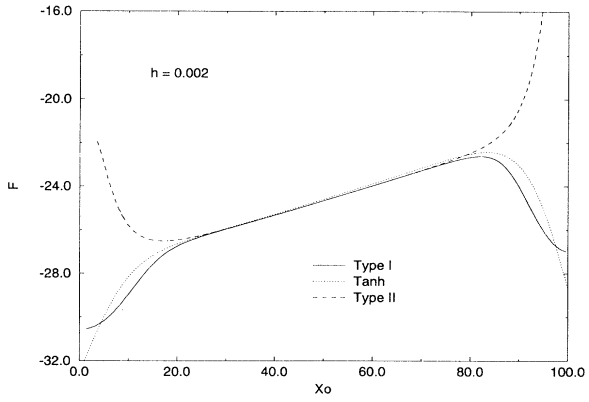

FIG. 4. Effective free energy as a function of the collective coordinate (position of the node in the order parameter profile) showing, for comparison, the free energy for the hyperbolic tangent trial function. In all cases $h = 0.002$.

For the case of fixed boundary conditions, i.e., type II, the free energy has a minimum at some point close to the higher temperature side, and therefore the kink moves towards that point from any initial position. The free energy for this type of boundary conditions is also shown in Fig. 4.

Finally, also shown in Fig. 4 is the free energy calculated for configurations of the order parameter given by the trial function (3.5) for varying x_0. As can be seen, the two curves obtained dynamically with differing boundary conditions coincide in the region away from the boundaries, which shows that the dynamics of the kink will not be affected by the boundary conditions until the kink comes within a few correlation lengths of the boundaries. The curve obtained from the local temperature solution (3.5) is also very close to the others in the region away from the boundaries.

To compare with the analytical results of Eq. (2.18), we computed the value of $dF[x_0]/dx_0$ for small values of h, in the region far from the boundaries, which is where the approximate analytical results are expected to hold. The numerical and analytical results for the slope of the effective free energy of the interfacial configuration agree within 2%. As shown in (3.3) the velocity of the interface is expected to be proportional to the gradient. Our numerical simulations yield the coefficient within 2–3 % of the approximate analytic result. We conclude that as long as the system size is sufficiently large (here ten correlation lengths is seen to be large enough), the trial function provides a semiquantitative description of the statics and relaxational dynamics.

IV. CONCLUDING REMARKS

In this short paper we have considered the statics and nonconserved relaxational dynamics of a two-phase interface in which the system is subjected to a temperature gradient. For the statics one has to extremize the free energy; a nonlinear change of variables preserves translational invariance and yields a representation in which the interface shape becomes equivalent to the time trajectory of a ball rolling in a potential, but slowed by friction [Eq. (2.8)].

It is seen that the temperature gradient couples to the "translation" mode of the unperturbed (isothermal) interface, so that perturbation theory can be applied to the introduction of the temperature gradient only if the mode is clamped by the finite size of the system. Even then the clamping is exceptionally weak for large systems, and the "linear response" is divergent, but correctly predicts which side of the sample will contain the interface. In realistic terms perturbation theory has vanishing domain since the effective coupling becomes $\sim h\exp(l)$, where h is a measure of the gradient and l is a measure of the system size, in units of the correlation length. Hence full nonlinear solutions and dynamical simulations were carried out numerically.

The equilibrium configurations are sensitive to the boundary conditions. For type I boundary conditions in which the order parameter derivative vanishes at the walls, the global equilibrium is for the system to remain in one phase. A single-kink extremum is argued to be a saddle point in the space of functions satisfying these boundary conditions. Simulations using relaxational (Langevin) dynamics reveal that an initial interface travels to one of the walls and the interface disappears. An interesting feature is that, generally, the interface travels toward the hotter wall at approximately constant velocity; however, if the initial interface is established close enough to the colder wall, it is removed there.

For "topological" boundary conditions (type II) in which the order parameter is forced to be in two different phases at the ends of the system, the equilibrium configuration has the interface near the hotter wall, which is consistent with the behavior of the free energy.

The structure of the free energy in the space of single kink configurations has been analyzed approximately using trial functions which should be accurate as long as the system size is sufficiently larger than the thermal correlation length. Good numerical agreement is found with purely numerical relaxational dynamics. The trial function along with assumed relaxational dynamics yields analytic results for the equation of motion of the interface position (collective coordinate), also in good agreement with purely numerical simulations.

For an order parameter with conserved (say, model B [8]) dynamics the situation is different. A configuration with a single interface cannot change much in response to a temperature gradient. However, a kink-antikink pair, representing a slab or bubble of one phase in the other, can move significantly while respecting the conservation. This topic is beyond the present scope and will be explored elsewhere.

ACKNOWLEDGMENTS

D.B. thanks H. J. de Vega for illuminating discussions, and he is grateful to the National Science Foundation for support under Grant Nos. PHY-93-02534 and INT-9016254 (Binational Collaboration with Brazil). F.T. has been supported by CNPQ and thanks the Department of Physics and Astronomy of the University of Pittsburgh for its hospitality. D.J. and J.L. are grateful to the Microgravity Science and Applications Division of NASA for support of the work under Grant No. NAG3-1403.

APPENDIX A: FORMAL SOLUTION OF THE LINEAR RESPONSE

The perturbation η_1 satisfies Eq. (2.13). Now, η_0 is a function of $Z = z - l/2$, so η_1 is also a function of this variable. As noted in the text, the function $\delta_1(Z) = \dot{\eta}_0(Z)$ is an eigenfunction of the second order fluctuation operator with eigenvalue zero. With this solution we can construct another linearly independent solution with unit Wronskian. Thus we find the following solutions of the homogeneous equation:

$$\delta_1(Z) = \dot{\eta}_0(Z) \ ,$$
$$\delta_2(Z) = \delta_1(Z)\int_0^Z \frac{dZ'}{\delta_1^2(Z')} \ . \tag{A1}$$

The zero mode $\delta_1(Z)$ is a symmetric function around $Z = 0$ and vanishes (linearly) at $Z = \pm l/2$. This motivates the choice of the lower limit in (A1), since now $\delta_2(Z)$ is antisymmetric around $Z = 0$ and obviously finite at $Z = \pm l/2$. Finally, the solution to Eq. (2.13) is

$$\eta_1(Z) = 3\delta_1(Z)\int_0^Z dZ'\delta_1(Z')\delta_2(Z') - 3\delta_2(Z)\int_0^Z dZ'\delta_1^2(Z') + \alpha_1\delta_1(Z) + \alpha_2\delta_2(Z) \tag{A2}$$

with constants $\alpha_{1,2}$ to be determined by the boundary conditions. Expanding the set of type I boundary conditions to linear order in h (and accounting for the explicit h dependence of the variable Z), one finds that the boundary conditions are symmetric around $Z = 0$, and since $\delta_2(Z)$ is antisymmetric, the coefficient α_2 vanishes. (This is a bonus of the parametrization in terms of Z and the choice of lower limit of the integrals in the functions above.) This indicates that the position of the interface is shifted; analyzing the behavior near $Z \simeq 0$ yields Eq. (2.14).

APPENDIX B: UNPERTURBED KINK

In a finite box the solution of Eq. (2.8) for $h = 0$ may be found by quadratures in terms of the elliptic sine function [11]

$$\eta_0(z) = \eta_i \mathrm{sn}[u|m] ,$$
$$u = \left(z - \frac{l}{2}\right)\sqrt{\frac{2-\eta_i^2}{2}} ,$$
$$m = \frac{\eta_i^2}{2-\eta_i^2}, \tag{B1}$$

where $\eta_0(0) = -\eta_i = -\eta_0(l)$ gives the values at the end points of the interval. The requirement that there is only one node in the interval is equivalent to requiring that the half-period of this solution be identified with l. This requirement in turn determines the value of η_i from the relation

$$K(m) = \frac{l}{2}\sqrt{\frac{2-\eta_i^2}{2}} \tag{B2}$$

in which $K(m)$ is the elliptic integral of the first kind [11] and is a quarter period of the elliptic function sn. This solution is a function of $Z = z - l/2$, and it obeys $\dot{\eta}_0(Z)|_{Z=-l/2} = \dot{\eta}_0(Z)|_{Z=l/2} = 0$.

[1] V. G. Levich and V. S. Krylov, Ann. Rev. Fluid. Mech. **1**, 293 (1969).

[2] See, e.g., R. S. Subramanian, in *Transport Processes in Bubbles, Drops and Particles*, edited by R. P. Chhabra and D. De Kee (Hemisphere, New York, 1992), pp. 1–42.

[3] A. Thess and S. A. Orszag, Phys. Rev. Lett. **73**, 541 (1994), and references cited therein.

[4] S. Brazovskii, in *Charge Density Waves in Solids*, edited by L. P. Gorkov and G. Gruner (North Holland, New York, 1989), p. 425.

[5] See, for example, Y. Lu, *Solitons and Polarons in Conducting Polymers* (World Scientific, New Jersey, 1988).

[6] See, for example, *Solitons and Condensed Matter Physics*, edited by A. R. Bishop and T. Schneider (Springer-Verlag, Berlin, 1978).

[7] G. Gruner, *Density Waves in Solids* (Addison Wesley, Reading, MA, 1994), p. 108.

[8] P. C. Hohenberg and B. I. Halperin, Rev. Mod. Phys. **49**, 435 (1977).

[9] E. L. Ince, *Ordinary Differential Equations* (Dover, New York, 1944), Chap. 14, p. 317.

[10] R. Rajaraman, Phys. Rep. **21C**, 229 (1975); R. Rajaraman, *Solitons and Instantons* (North Holland, Amsterdam, 1984).

[11] P. F. Byrd and M. D. Friedman, *Handbook of Elliptic Integrals for Engineers and Scientists* (Springer-Verlag, Berlin, 1971).

[12] M. Abramowitz and I. A. Stegun, *Handbook of Mathematical Functions* (Dover, New York, 1970).

[13] David Jasnow, in *Phase Transitions and Critical Phenomena*, edited by X. Domb and X. Green (Academic, City, 1986), Vol. 10, p. 269.

[14] J. Rudnick and D. Jasnow, Phys. Rev. B **24**, 2760 (1981).

[15] J. L. Gervais and B. Sakita, Phys. Rev. D **11**, 2943 (1975).